

**FLUID AND PARTICLE LASER DOPPLER VELOCITY
MEASUREMENTS AND MASS TRANSFER PREDICTIONS FOR
THE USP PADDLE METHOD DISSOLUTION APPARATUS.**

L.M. Bocanegra,
Facultad de Ingenieria, Universidad Nacional de Trujillo,
Aparatado 315, Trujillo, Peru,
G.J. Morris and J.T. Jurewicz,
Department of Mechanical Engineering, West Virginia University,
Morgantown, WV 26506
J.W. Mauger,
College of Pharmacy, University of Nebraska,
42nd and Dewey Ave., Omaha, Nebraska 68105-1065.

ABSTRACT

This research was motivated by the lack of experimental data concerning the complex flow fields produced by the USP Paddle Method Dissolution Test Apparatus, which influence the reproducibility and sensitivity of the resulting dissolution data.

A one-component He-Ne fiber optics laser Doppler anemometer and a conditional sampling computer data acquisition provided unique three-dimensional fluid velocity measurements in most regions of the fluid inside the vessel. Tangential velocities which are predominant in magnitude decrease as a function of distance from the paddle to the liquid surface. Low magnitude circulation patterns in the axial direction exist with

little interaction between the fluid above and below the paddle. The radial velocity component also exhibits a low magnitude. In the vicinity of the paddle, a periodic fluid motion produced by the wake formed behind the paddle exists. Close to the bottom of the vessel, tangential fluid velocities were approximately equal to solid body rotation created by the paddle, and make possible predictions of mass transfer rates from a non-disintegrating calibrator resting at the bottom of the vessel.

The motion of drug particles from a dissolving tablet was simulated by using 216 μm diameter polystyrene latex spheres. They provided the Stokes number matching an average drug particle diameter of 190 μm . Tangential particle velocity measurements taken at selected locations using two different paddle speeds (50 and 60 RPM) revealed that the particles closely followed the fluid. A comparison between the fluid and the particle tangential velocities at 50 and 60 RPM showed that for 60 RPM the particle to fluid relative velocity above the paddle increased by about 100%, with the mass transfer rate in that region predicted to be enhanced by 37%.

INTRODUCTION

Tablets represent a convenient drug delivery system with the release mechanism of the active drug ingredient being initiated with the disintegration of the tablet into smaller

fragments. When these fragments are exposed to the aqueous environment of the gastrointestinal tract, drug dissolution begins. Therefore, drug dissolution is a precursor to drug absorption and in-vitro dissolution testing can be rationalized as being an indicator of dissolution kinetics for a particular tablet formulation.

One of the official methods for testing dissolution properties of drug solid forms is the United States Pharmacopeia (USP) Paddle Method (or method II). Prasad *et al.*¹ carried out dissolution experiments using two prednisone formulations: the USP prednisone calibrator and the National Center for Drug Analysis (NCDA) prednisone standard. Tests were made under normal and perturbed operating conditions (i.e., eccentricity and/or tilt of the axis of the paddle). Under normal operating conditions both standards produced similar dissolution results; however, for the perturbed case, the NCDA standard produced different results compared to the USP calibrator. The basic reason for this difference cannot be fully understood unless the hydrodynamic behavior inside the USP dissolution vessel is known. Several hydrodynamic studies for flat bottom tanks are available in the literature²⁻⁵, but are not directly applicable to the USP apparatus.

The importance of the hydrodynamics of the system is linked with the mechanism of dissolution from a drug particle.

Dissolution is due to a convective diffusion mechanism related to localized shear at the particle surface. Both the sensitivity and the reproducibility of the resulting dissolution data will depend on the velocity profile for each component of flow, velocity gradients, circulation patterns, and stability of flow. Thus, measurement of fluid flow phenomena within the USP dissolution vessel is required in order to evaluate dissolution performance.

A fiber optics laser Doppler anemometer measures instantaneous fluid velocities for each component of flow without perturbing the native characteristics of the flow field.

The objective of this study was to characterize the flow inside the USP dissolution vessel (paddle method) by measuring instantaneous fluid and simulated drug particle velocities within the dissolution vessel. Measurements were taken by using a fiber optics laser Doppler anemometer at zones above, below, and at the level of the paddle. Paddle speeds of 50 and 60 RPM were considered and the resulting data is useful in understanding the complex hydrodynamic behavior inside the USP dissolution vessel (paddle method) and in comparing the effect of different stirring speeds on predicted mass transfer coefficients.

EXPERIMENTAL

Test Conditions. The paddle was positioned (relative to the vessel) according to the specifications of the USP XXI⁶

dissolution standards. For most of the testing, a 50 RPM paddle speed was used and in order to be able to study the effect (on the flow) of a higher speed of rotation, velocity measurements for selected locations were taken at 60 RPM. All of the runs were made using 900 ml of water.

Experimental Set-Up. A one-component DANTEC fiber optics laser Doppler anemometer (FOLDA) and a conditional sampling device were interfaced with a microcomputer as shown in Figure 1. Details concerning the operation principle of the FOLDA appear in the Appendix. A 15 mW He-Ne laser beam was sent to the optical components and split into two equal intensity beams with orthogonal axis of polarization and frequency shifted with respect to the other by 40 MHZ. These beams traveled together along a 4 μ m core diameter fiber optics cable and were separated at the FOLDA probe head and their crossing point positioned at the fixed spatial location where velocity measurements were intended (measuring volume). The intensity of the scattered light from particles crossing the measuring volume was collected by a photomultiplier tube and its frequency information sent to the counter processor and microcomputer for further processing.

The conditional sampling device consisted of an electronic circuitry, a one-slot light chopper rotating with the shaft, and an IR emitting diode and photodetector interfaced with the microcomputer. Through this device it was possible to correlate the angular position of the paddle relative to the measuring

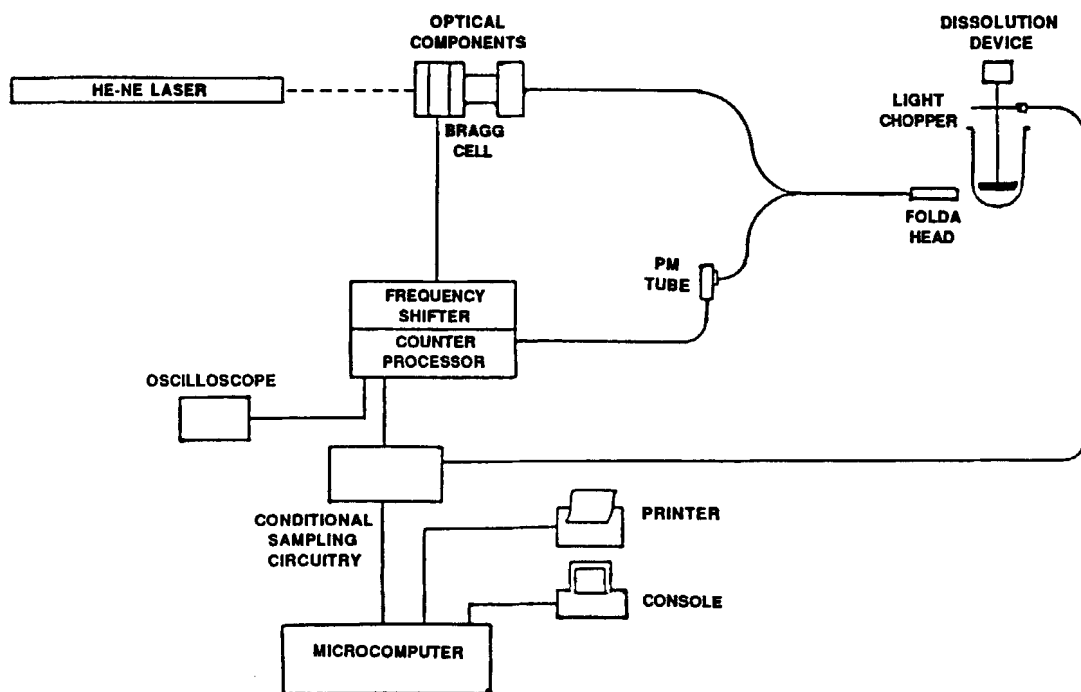


Figure 1: Data acquisition system block diagram.

volume (PRP) and to generate a velocity time history for a fixed spatial point as the paddle rotated. Because the particles would cross the measuring volume at random times, thus producing a random data arrival, the data collected for a revolution of the paddle were sorted into forty intervals or "bins". Since the period of revolution was constant, data for each bin were collected over a number of revolutions that would provide statistically meaningful data.

Particles used. Because a clean fluid (*i.e.*, distilled water) is free of particles, laser Doppler anemometer velocity measurements are not possible unless particles are added to the fluid. Four micron diameter metallic coated glass beads (TSI mod. 10087) were added into the fluid to track its motion accurately. Particles resulting from the tablet fragments during the dissolution process experience shape and size variations through time; and for particle velocity measurement purposes, their motion was simulated by using 216 μm diameter polystyrene latex spheres ($\rho=1.03 \text{ gm/ml}$) which matched the Stokes number and resembled the particle dynamics of 190 μm average mean diameter drug particles ($\rho=1.35 \text{ gm/ml}$).

RESULTS AND DISCUSSION

Laser Visualization Studies. Laser flow visualization studies focused on horizontal and vertical planes above and below the paddle. A representation of the major components of the flow as determined from those studies is shown in Figure 2. Fluid flow is generated by the momentum transfer from the paddle via normal stresses. In the region above the paddle, a major component of flow is tangential, which leads to circular fluid motion. This fluid pattern is shown by vectors directed outward from the paper. In the axial direction a rotational secondary flow was observed and is represented by the reversed direction of the vertical arrows. This component of the flow results in an oscillation in the axial component of the flow, which has not

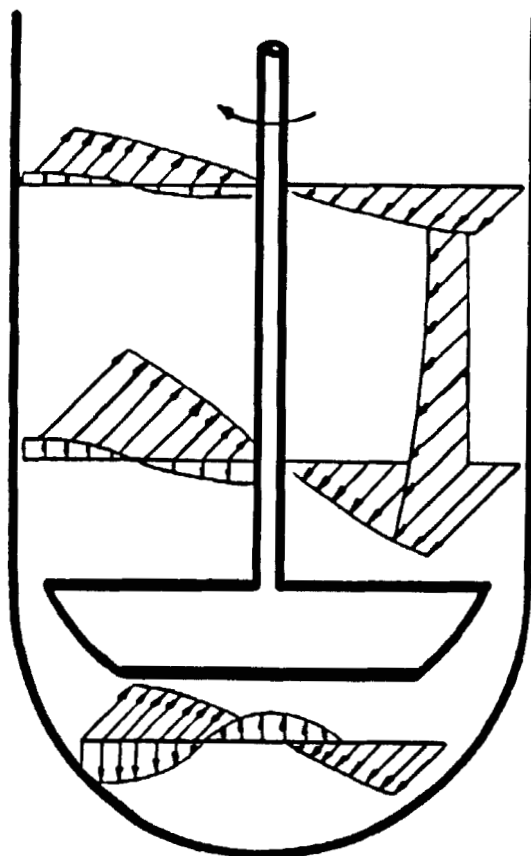


Figure 2: Fluid flow field from a laser flow visualization for the USP paddle dissolution device.

been previously reported, and is of potential importance to the sensitivity and reproducibility of resulting dissolution data

level of the paddle and below the paddle. All of the velocity data has been normalized to the paddle tip speed. Also, geometrical parameters have been normalized. The height of the fluid level (76 mm) measured from the plane where the hemispherical bottom develops and the maximum radius of the hemispherical bottom (50.8 mm) for the axial and radial directions, respectively, have been used in the normalization process.

Figure 3 shows the normalized (dimensionless) coordinate system used. The velocity data is plotted as a function of the angle between the paddle and the measuring volume (paddle relative position, PRP). Figure 4 presents tangential velocity data at a plane just above the paddle ($Z = -0.066$) and it is seen that a 180° periodic tangential velocity produced by the two bladed paddle exists and velocities decreased as the paddle approached the measuring volume (PRP of 0° and 180°) and increased as it left the measuring volume. Close to the bottom of the vessel ($Z = -0.605$) velocities were approximately equal to that of the paddle (Figure 5), thus making possible mass transfer predictions from a non-disintegrating tablet resting at the bottom of the vessel.

Figure 6 presents axial velocity data for $Z = -0.066$ and for a curve corresponding to the same radius, upward motion (positive values) and downward motion (negative values) exist. Also, this velocity component exhibits a 180° periodicity and

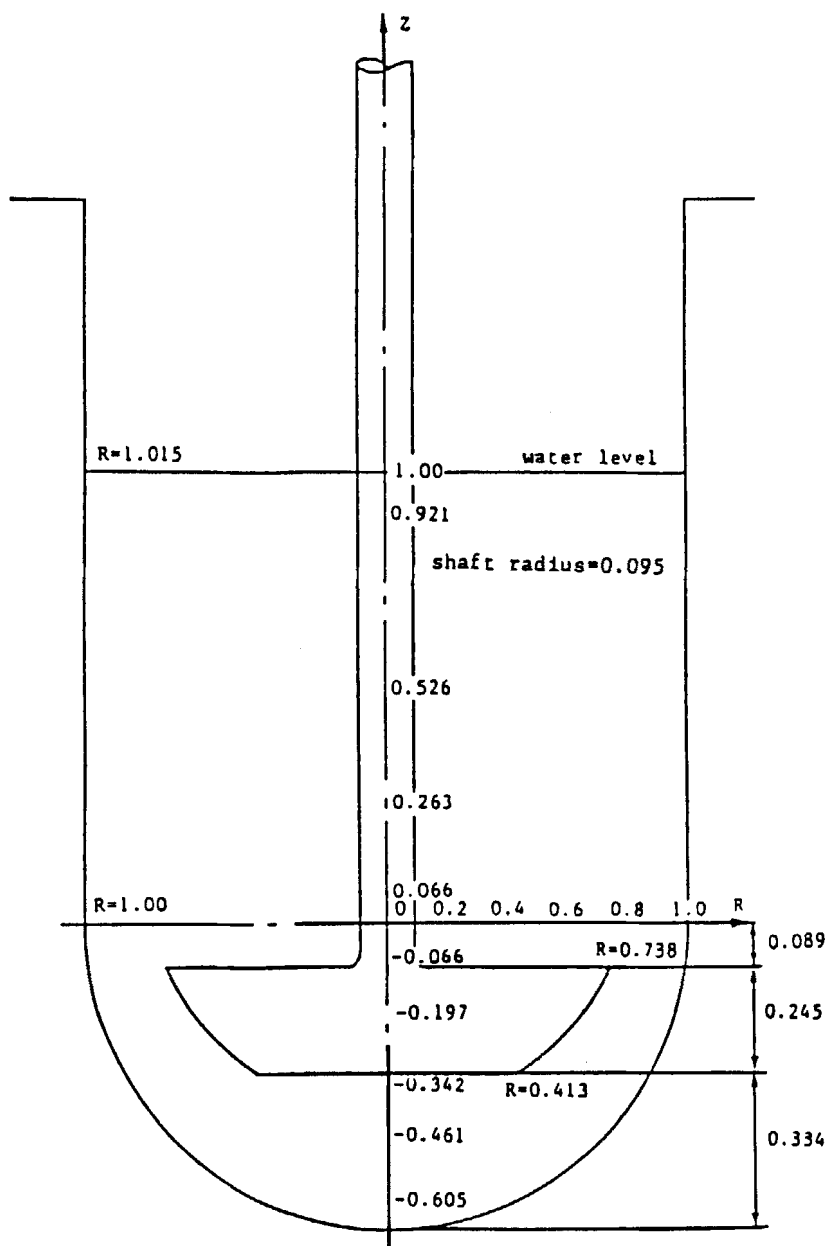


Figure 3: Normalized coordinate system used for the USP dissolution vessel: $R=r/r_w$, $r_w=50.8$ mm; $Z=z/z_1$, $z_1=76$ mm.

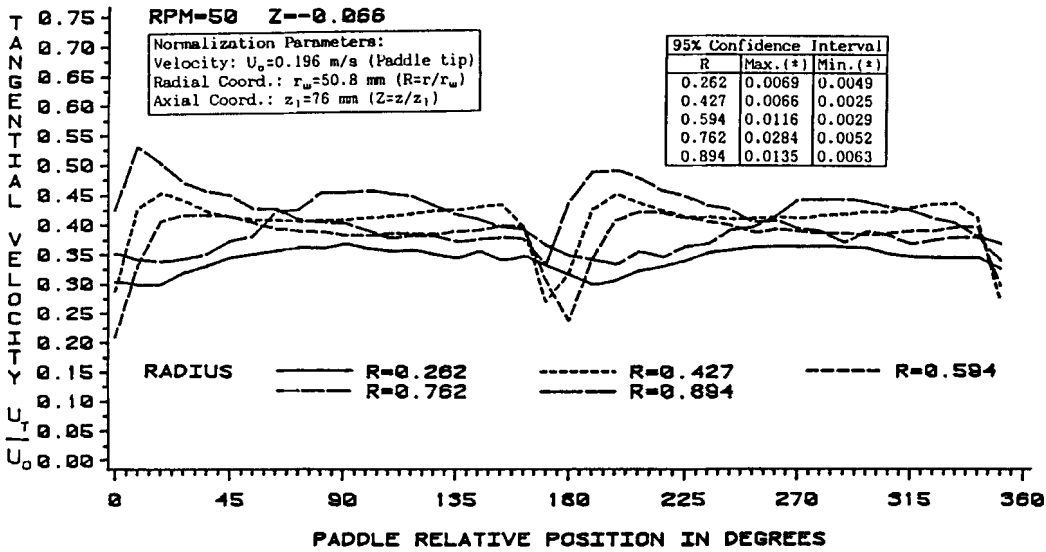


Figure 4: Tangential fluid velocity versus paddle relative position at plane $Z=-0.066$. Parameter: R , normalized radial coordinate of the measuring volume.

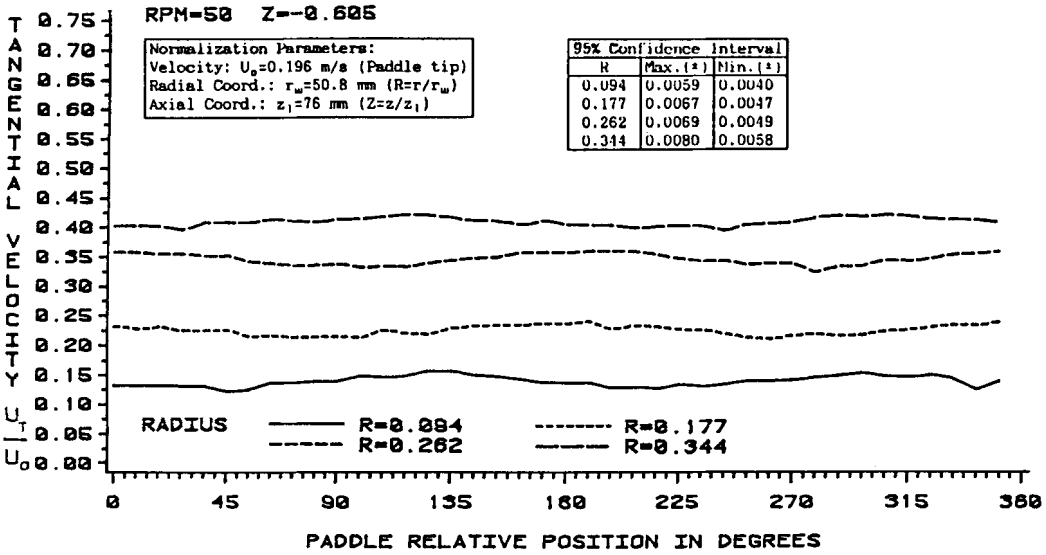


Figure 5: Tangential fluid velocity versus paddle relative position at plane $Z=-0.605$. Parameter: R , normalized radial coordinate of the measuring volume.

Drug Development and Industrial Pharmacy Downloaded from informahealthcare.com by Biblioteca Alberto Malliani on 01/27/12
For personal use only.

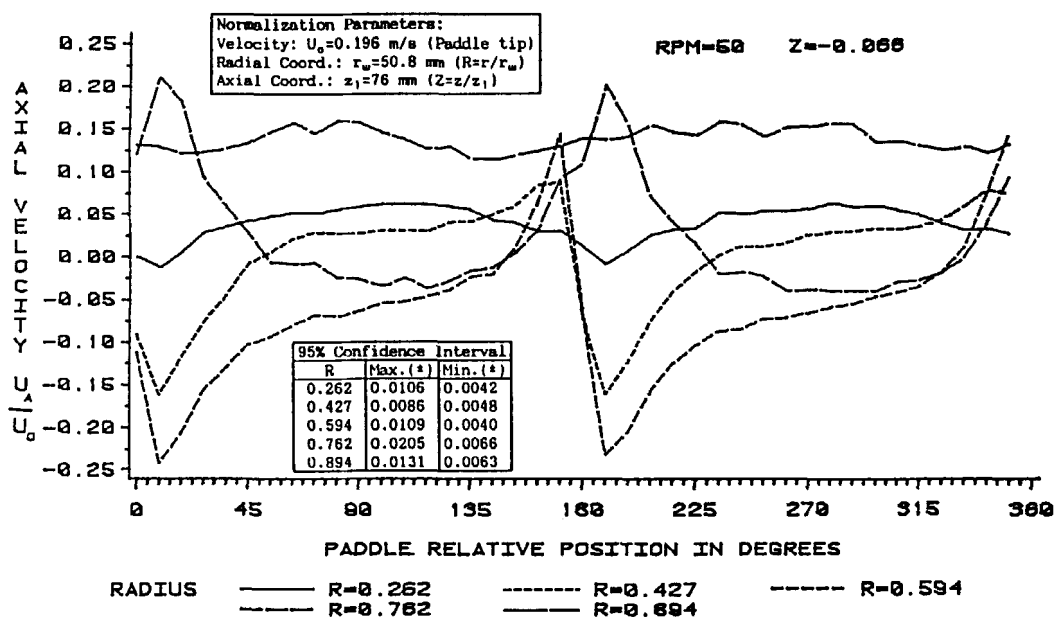


Figure 6: Axial fluid velocity versus paddle relative position at plane $Z = -0.066$. Parameter: R , normalized radial coordinate of the measuring volume.

lower velocity magnitudes when compared to the tangential velocity component.

Figure 7 presents radial velocity data below the paddle ($Z = -0.461$) and it is characterized by its 180° periodicity and low magnitude with positive values that indicate motion towards the wall of the vessel. The author's conception of the flow on the vertical plane of the paddle is presented in Figure 8 (7). The flow at the level of the paddle is discharged towards the wall and then divides into upward and downward

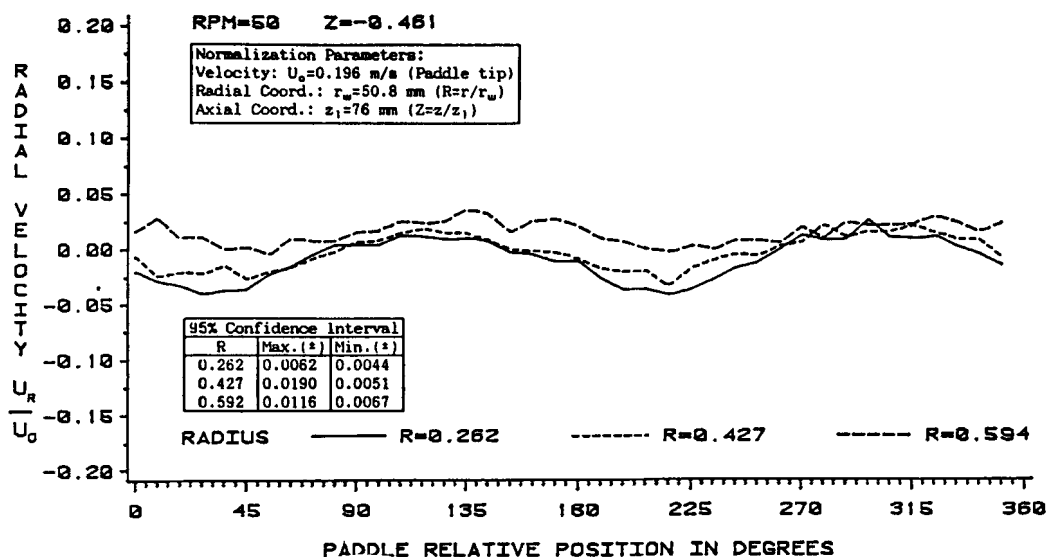


Figure 7: Radial fluid velocity versus paddle relative position at plane $Z=-0.461$. Parameter: R , normalized radial coordinate of the measuring volume

moving streams. Above the paddle two circulation patterns occur with upward fluid motion close to the surface of the shaft and close to the wall and with downward fluid motion for intermediate radii. Below the paddle it is seen that the fluid moves downwards parallel to the wall and also establishes a circulation pattern. Because of the low velocity magnitudes in the axial direction, mixing is not enhanced between the zones above and below the paddle and particles above and below the paddle, may experience oscillatory motion.

Particle Velocity Measurements. In this section a comparison between fluid and particle velocities (polystyrene beads were

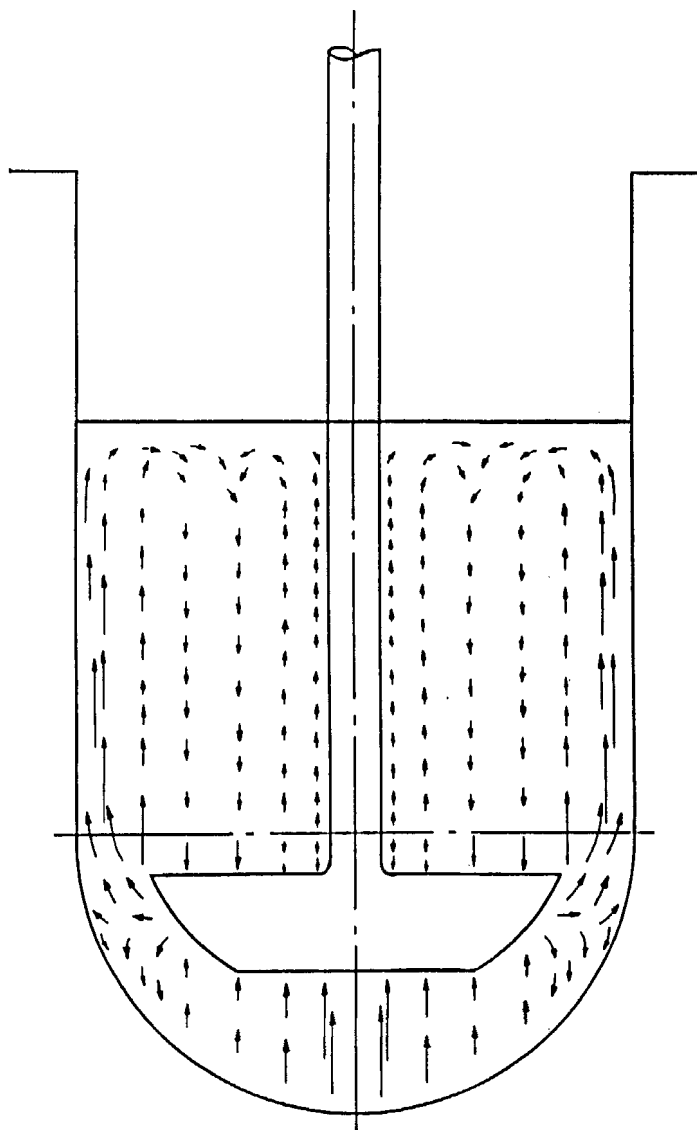


Figure 8: Author's conception of an instantaneous flow pattern at the vertical midplane of the paddle.

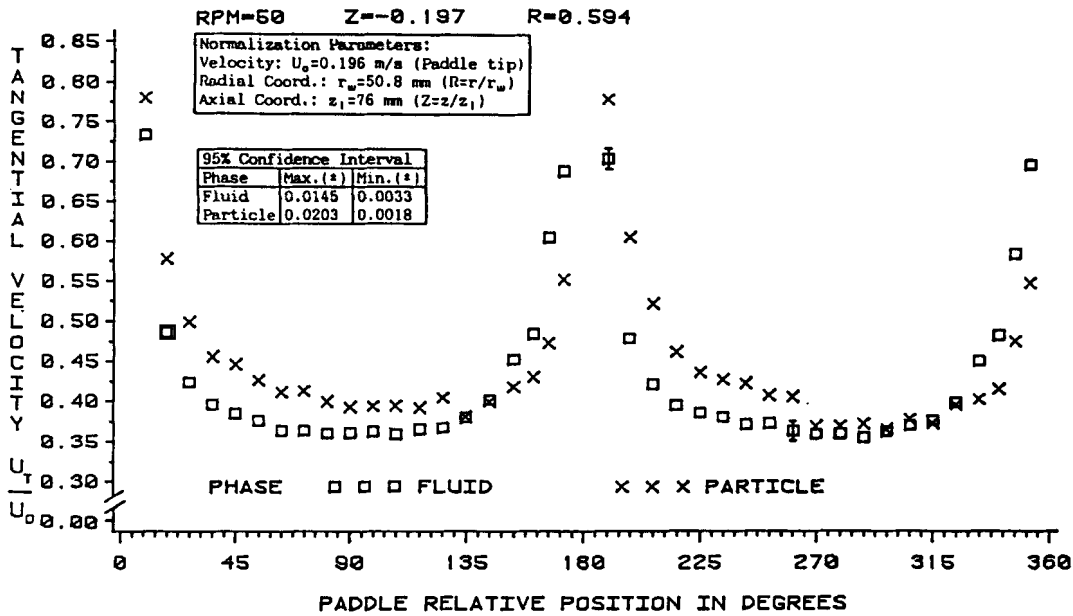


Figure 9: Comparison between tangential fluid velocity and tangential particle velocity as a function of paddle relative position at the level of the paddle for $Z=-0.197$ and $R=0.594$ at 50 RPM.

used to simulate the particle dynamics of drug particles).

Particle velocity measurements were taken above, below and at the level of the paddle for $R=0.594$ at 50 and 60 RPM. Figure 9 presents particle and fluid velocity data at the level of the paddle ($Z=-0.197$) for 50 RPM. It is seen that as the paddle approaches the measuring volume (PRP=180°) the particles lag the flow and after the paddle crosses the measuring volume, the particles exhibit a higher velocity with respect to the fluid and it is attributed to the fact that the particles take a

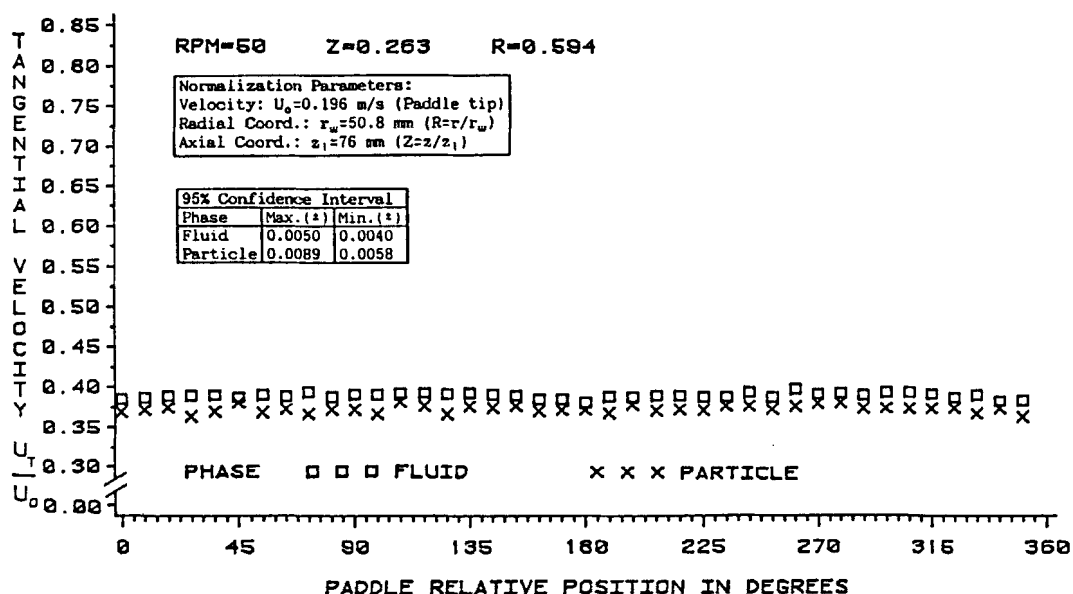


Figure 10: Comparison between tangential fluid velocity and tangential particle velocity as a function of paddle relative position below the paddle for $Z=0.263$ and $R=0.594$ at 50 RPM.

longer time to adjust to the changes introduced by the paddle. These differences in velocity between the fluid and the particle reveal that the mass transfer process takes place by a convective diffusion mechanism. Figures 10 and 11 present data above the paddle ($Z=0.263$) at 50 and 60 RPM, respectively. From these figures it is seen that for 60 RPM there exists a larger velocity difference between the fluid and the particles, which would result in increased mass transport rates in this region.

Dissolution Rate Predictions near the bottom of the Vessel.

Relating flow regime characteristics for the USP paddle dissolution method to dissolution performance is an important

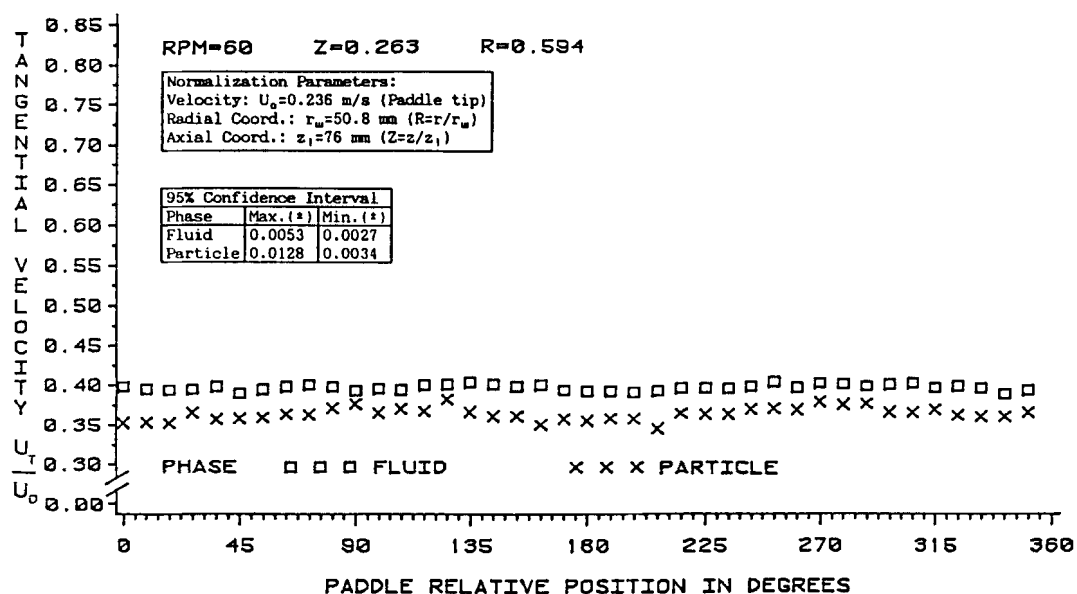


Figure 11: Comparison between tangential fluid velocity and tangential particle velocity as a function of paddle relative position above the paddle for $Z=0.263$ and $R=0.594$ at 60 RPM.

outcome for the experimentally determined fluid dynamics data.

Data from this study show that the tangential velocity component of the fluid predominates, and that flow near the bottom of the vessel is approximately equal to solid body rotation. Thus, fluid velocity in this region is approximated by solid body rotation via ωr where ω is the angular velocity of the paddle and r is the radial distance along the paddle.

Colton and Smith⁸ have discussed a mass transport model for a fluid undergoing solid body rotation above a stationary non-disintegrating disk. As noted by these authors, an idealized

representation is one where the fluid core outside the boundary layer occurs as solid body rotation with angular velocity $\gamma\omega$, $0 < \gamma < 1$ where γ is a dimensionless ratio of angular velocity in the fluid to impeller angular velocity. More recently, Khoury⁹ *et al.* have demonstrated the utility of a similar model applied to mass transfer systems of pharmaceutical interest described by the equation below.

$$R = 0.77 D^{2/3} \nu^{-1/6} (\omega\gamma)^{1/2} A C_s \quad (1)$$

Where R is the dissolution rate (g/sec), D is the diffusion coefficient for the dissolving species (cm^2/sec), ν is the kinematic viscosity of water (cm^2/sec), ω and γ are quantities previously defined, A is the area of the disk (cm^2), and C_s is the solubility of the dissolving material (Gm/ml). This expression is valid when ν/D is large, which is true for solutes such as salicylic acid dissolving in aqueous media where the magnitude is approximately 10^3 .

The USP procedure for salicylic acid calibrator tablets requires the determination of amount of salicylic acid dissolved at thirty minutes for each spindle, expressed as percent of the labeled amount. Conditions require using 900 ml of 0.05M phosphate buffer pH 7.40, with the dissolution test run at 37 degrees Centigrade.

Under conditions of 0.05M phosphate buffer at pH 7.40, salicylic acid solubility at the face of the dissolving disk is influenced by the pH of the buffer in the bulk and the self

buffering capacity of the dissolving salicylic acid¹⁰. From measured pH values for phosphate buffers saturated with salicylic acid, the pH at the dissolving surface is estimated to be 3.41, with a corresponding solubility of 0.07M (0.01 g/ml)¹¹.

Thus for a salicylic acid disk with a radius of 0.48 cm having one side exposed for dissolution the expected dissolution rate is:

$$R = 0.77 (1.13E-05)^{2/3} (6.99E-05)^{-1/6} (\omega 0.95)^{1/2} (0.48)^2 (0.01)$$

$$R(50RPM) = 1.4E-05 \text{ g/sec}$$

$$R(100 \text{ RPM}) = 2.0E-05 \text{ g/sec.}$$

A value of 0.95 was chosen for γ based on the observed fluid velocity data. A recent calibrator set (lot I) specifies suitability ranges for the paddle apparatus as 2.0E-05 to 3.7E-05 g/sec at 50 RPM and 3.0E-05 to 4.7E-05 g/sec at 100 RPM. Average dissolution rate data determined under USP conditions for this lot were found to be 2.7E-05 g/sec at 50 RPM and 3.7E-05 g/sec at 100 RPM. These values are approximately two times greater than the calculated values, which is anticipated since the actual data reflect dissolution from two faces.

Therefore, it appears feasible under conditions of known flow regime to estimate dissolution rates from nondisintegrating disks. A more exacting test requires experimental dissolution data from disks having an impermeable cover on the bottom side so that dissolution occurs only from the side facing the stirred liquid.

Effect of the Speed of Rotation on the Predicted Average Local Mass Transfer Coefficient. Using the experimental particle and fluid average velocity data for $Z=0.263$ and $R=0.594$ (Figures 10 and 11) in Equation 2¹² for a salicylic acid particle dissolving in water by a convective-diffusion mass transfer process the ratio between the predicted local mass transfer coefficients at 50 and 60 RPM is calculated below. In Equation 2, k is the mass transfer coefficient (cm/s), d_p is the particle diameter, D is the diffusion coefficient (cm²/sec), v_{rel} is the average velocity of a particle with respect to the fluid (cm/s), and ν is the kinematic viscosity.

$$\frac{k d_p}{D} = 2.0 + \left| \frac{d_p v_{rel}}{\nu} \right|^{0.5} \left| \frac{\nu}{D} \right|^{0.33} \quad (2)$$

For $v_{rel1} = 3.38 \times 10^{-3}$ m/s (at 50 RPM)

$v_{rel2} = 7.98 \times 10^{-3}$ m/s (at 60 RPM)

Results $\frac{k_2}{k_1} = 1.37$

This result reveals that the predicted mass transfer coefficient at $Z=0.263$ and $R=0.594$ is expected to be enhanced when the RPM are increased by 20%.

CONCLUSIONS

This study has demonstrated the usefulness of a fiber optics laser Doppler anemometer as an unobtrusive method to map the flow field for the USP paddle dissolution method. Fluid velocity measurements have been made for the tangential,

radial, and axial components of flow in various regions throughout the vessel.

Relevant to dissolution testing is the finding that periodicity in the tangential velocity component near the paddle is damped at the bottom of the vessel. Thus, solid dosage forms dissolving from the bottom are subjected to shear caused by predictable and stable flow with a paddle speed of 50 RPM. Knowledge of this flow regime makes feasible the prediction of dissolution rates from nondisintegrating salicylic acid disks.

Circulation patterns above and below the paddle were developed from an analysis of the axial and radial components of the flow. These patterns are weak compared with tangential velocities and demonstrate that optimal mixing is not predicted between zones below and above the paddle.

For particles suspended in the bulk, particle velocities lag the fluid velocity. Therefore, drag occurs across the surface of the particle and dissolution rates would be sensitive to fluid velocity and direction.

ACKNOWLEDGEMENTS

The authors are thankful to the Upjohn Company for providing an equipment grant to purchase the fiber optics laser Doppler anemometer. Dr. Luis Bocanegra wishes to express his thanks to The United States Pharmacopeial Convention for providing support by awarding him with two one-year fellowships.

REFERENCES

1. V. Prasad, V. Shah, J. Hunt, E. Purich, P. Knight and B. Cabana, J. Pharm. Sci., 72, 42 (1983).
2. S. Nagata, "Mixing Principles and Applications," New York: John Wiley (1975).
3. J. Bertrand, J.P. Couderc and H. Angelino, Chem. Eng. J., 19, 113 (1980).
4. M. Yianneskis, Z. Popiolek and J. Whitelaw, J. Fluid Mech., 175, 537 (1987).
5. M.E. Chudacek, Chem. Engineering Science, 40, 385 (1985).
6. The United States Pharmacopeia, 21st Rev., Mack Publishing Co., Easton, PA, 1243 (1985).
7. L.M. Bocanegra, "A Two-Phase Flow Experimental Study of the United States Pharmacopeia Paddle Method Dissolution Test Apparatus", Ph.D. Dissertation, West Virginia University (1988).
8. C.K. Colton and K.A. Smith, AIChE J., 18, 949 (1972).
9. N. Khoury, J. Mauger and S. Howard, Pharmaceutical Research, 5, 495 (1988).
10. D. McNamara and G. Amidon, J. Pharm. Sci., 77, 511 (1988).
11. Z. Ramtolla and O.I. Corrigan, Drug Development and Industrial Pharmacy, 13, 1703 (1987).
12. E.L. Cussler, "Diffusion Mass Transfer in Fluid Systems," New York: Cambridge University Press (1984).

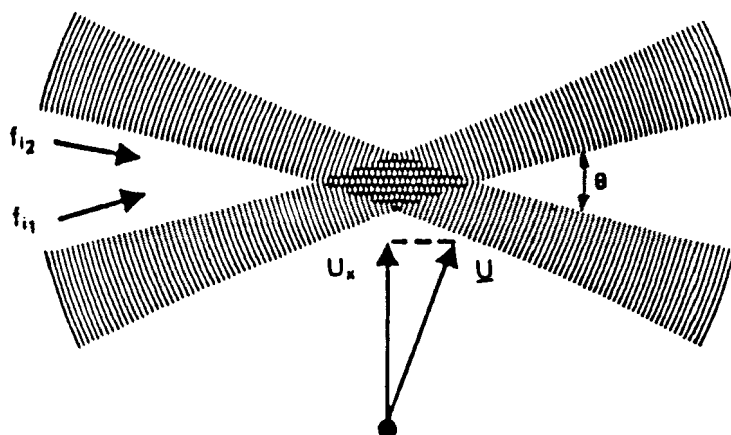


Figure A.1: Illustration of the fringes produced by the intersection of two coherent and monochromatic laser beams.

APPENDIX: Operation Principle of the Laser Doppler Anemometer

When two coherent and monochromatic light waves intersect at an angle they create interference patterns (fringes) which can be explained by the principle of superposition of oscillations. The resultant of the light intensity is obtained from the sum of two electromagnetic wave fields, and appearing regions of maxima and minima light intensity are referred to as "bright" and "dark" fringes, respectively. (See Figure A.1).

Laser velocity measurements are taken at the point where the laser beams cross, known as *measuring volume*. A particle crossing such point will scatter light and its intensity can be collected by a photo-detector device. The frequency of the

scattered light provides information to calculate the velocity component in the direction normal to the fringes for a particle crossing the measuring volume and can be calculated from Equation A.1.

$$v_x = \delta f_d \quad (\text{A.1})$$

where the fringe spacing $\delta = \frac{\lambda}{2 \sin(\theta/2)}$,

and the angle θ is a function of the optical components used in the laser Doppler anemometer, and f_d is the frequency of the scattered light.